Advanced Probe Measurement System in TU-Heliac

Yutaka TANAKA, Hiromi TAKAHASHI, Hiroyasu UTOH, Michiaki OGAWA, Junji SHINDE, Hiroshi AOYAMA, Keisuke IWAZAKI, Hajime UMETSU, Atsushi OKAMOTO, Katsuhiro SHINTO, Sumio KITAJIMA, Masayuki YOKOYAMA[1)], Shigeru INAGAKI[1)], Yasuhiro SUZUKI[1)], Kiyohiko NISHIMURA[1)] and Mamiko SASAO

Department of Quantum Science and Energy Engineering, Tohoku University, Sendai, 980-8579, Japan
[1)]*National Institute for Fusion Science, Toki, 509-5292, Japan*

(Received 4 December 2006 / Accepted 31 March 2007)

An advanced probe measurement system consisting of high-speed Langmuir probes with a preamplifier and a Copper shield was designed and installed in TU-Heliac. Potential and density fluctuations were measured in the hot-cathode biased plasma, and power spectra were calculated using the complex Fourier transform. There were low frequency fluctuations ($f < 10$ kHz), high frequency fluctuations ($70 < f < 200$ kHz) and sharp spectra applied for the plasma production ($10 < f < 50$ kHz). In the region above 200 kHz, the power decreased by a factor of $1/f^2$ for the potential fluctuation and $1/f^{2\sim3}$ for the density fluctuation. The phase shift between potential and density fluctuations was almost 0 rad at $\rho = 0.54$. On the other hand, the phase shift was not 0 rad at $\rho = 0.21$, especially in the $100 \sim 200$ kHz region. The high frequency fluctuation at $\rho = 0.21$ grew on the time scale of 10^{-5} s, which was obtained from the time dependent signals of the high frequency fluctuation.

Keywords: heliac, electrode biasing, poloidal flow, fluctuation, instability

DOI: 10.1585/pfr.2.S1090

1. Introduction

With control of heating power, the transitions to the H-mode have been observed in many devices. The transition was discovered in the ASDEX tokamak in 1982 [1]. With regard to stellarators, the H-mode transition was observed in W7-AS [2], and recently the transition with a clear decrease in H_α emission was observed in CHS [3]. In small devices, electrode biasing is a useful method to drive and control the poloidal flow, and to study the improved mode transition. Biasing experiments have been carried out in many devices [4–6], and transitions to the improved mode were observed. In Tohoku University Heliac (TU-Heliac), negative biasing experiments using a hot-cathode electrode have been carried out [7–13]. Just after biasing the hot-cathode, the transition to the improved mode occurred, and formation of radial electric field (4 kV/m) and a threefold increase in line density were observed. Density fluctuations in the $10 \sim 100$ kHz range were suppressed. On the other hand, density fluctuations in the $100 \sim 300$ kHz had large power. It is important to clarify the mechanism of the fluctuations and instability in biased plasma. The Langmuir probe method, which has fine time and spatial resolutions, is useful to measure the fluctuation. In this study, an advanced probe measurement system, which was capable of measuring density and potential fluctuations up to 1 MHz, was designed and installed in the TU-Heliac. In addition, density and potential fluctuations were measured simultaneously in a hot-cathode biasing experiment.

author's e-mail: yutaka.tanaka@ppl2.qse.tohoku.ac.jp

2. TU-Heliac and High Speed Langmuir Probe

TU-Heliac is a small helical axis stellarator [13]. The toroidal period number N is 4, and the major radius R_0 is 48 cm. In this study, the standard configuration of TU-Heliac was selected. The minor radius a was 6.8 cm, the magnetic field B_0 was 0.3 T. The working gas was He, and its pressure was 1.2×10^{-2} Pa. The plasma was produced by low frequency ohmic heating ($f = 18$ kHz). The ohmic heating coils were wound outside the vacuum vessel like vertical field coils. The alternate plasma current was about 200 A. In the biasing experiment, a hot-cathode of LaB_6 was used. LaB_6 has a low work function of 2.7 eV. The hot-cathode was heated at about 1500°C, negatively biased against the vacuum vessel, and emitted thermal electrons. The typical electron temperature T_e and electron density n_e of the target plasma for biasing were < 25 eV and 5×10^{11} cm^{-3}, respectively. The typical electron temperature T_e and electron density n_e of the biased plasma were < 20 eV and 2×10^{12} cm^{-3}, respectively. Skin depth of the plasma at 18 kHz was 1~2 cm, and the plasma current flowed near the plasma surface. Absorbed heating power to the plasma estimated from the plasma current and the plasma resistivity was about 1 kW.

In the fluctuation measurement, the power spectrum and wavenumber of density and potential fluctuations are important to monitor the conditions of the fluctuation. To discuss the growth rate of the fluctuation, it is necessary to determine the phase shift between density and poten-

tial fluctuations. Fluctuations of ion saturation current I_s and floating potential V_f can be treated as those of density and space potential, respectively. In biased plasma in TU-Heliac, high frequency density fluctuation ($f > 100$ kHz) has been observed. Therefore, the cutoff frequency of the fluctuation measurement system should be up to 1 MHz. An I_s measurement circuit could be designed easily up to a cutoff frequency of 1 MHz, because we can select a low impedance resistor to measure the ion saturation current. On the other hand, the V_f measurement circuit should be designed carefully. In V_f fluctuation measurement, the plasma can be considered as an alternating voltage source with the output resistor R_f for the small amplitude fluctuation near $V_{bias} = V_f$, where V_{bias} is the bias voltage. R_f is written as:

$$R_f = \frac{dV_{bias}}{dI_{probe}}\Big|_{V_{bias}=V_f} , \quad (1)$$

where I_{probe} is the probe current. In the TU-Heliac plasma, R_f was $1 \sim 10$ k Ω. Therefore, the resistor to measure V_f within 1% error was 1 MΩ. The cutoff frequency of the V_f measurement system is dependent on $\omega = 1/R_f C_f$, where C_f is the stray capacity of the lead cable. To maintain the cutoff frequency 1 MHz, C_f was less than 10 pF, which was equivalent to 10 cm. Then, a 1 MΩ resistor was connected 10 cm behind the probe tip. A preamplifier immediately after the resistor was required to transmit the V_f signal with low output impedance. Outside the vacuum vessel, an isolation amplifier was required to reject common mode noise and transmit the signals to an oscilloscope. Figure 1 shows a schematic diagram of the fluctuation measurement system. We considered the V_f transmission path divided into 3 sections: the 1st section was from the V_f probe tip to the preamplifier, the 2nd section was from the preamplifier to the isolation amplifier, and the 3rd section was from the isolation amplifier to the oscilloscope. The lengths of the 1st, 2nd, and 3rd sections were about 10 cm, about 1.5 m, and about 25 m, respectively. In the fluctuation measurement, noise suppression is important to gain large dynamic range. A Cu tube was inserted in the 1st section as an electrostatic and electromagnetic shield. This Cu tube was connected to the vacuum vessel, and its thickness was 0.15 mm, which corresponded to the skin depth of Cu at 200 kHz. The operational amplifier (OPA627) was inserted as a unity gain buffer into the top of the 2nd section. This operational amplifier is characterized by high speed and low noise. A 50 MHz isolation amplifier was included at the top of the 3rd section. The sampling rate of the oscilloscope was 6 MS/s. To prevent the phase delay between the 4 signals, we adapted 4 co-axial cables of the same length between the 4-channel isolation amplifier and 4-channel oscilloscope. The total cutoff frequency of this system was 1 MHz. The thickness of the ion sheath is important for the arrangement of the probe tips. The Debye length λ_D was $\lambda_D = \sqrt{\varepsilon_0 T_e / ne^2} \sim 10^{-5}$m, and then the thickness of the ion sheath was 10^{-4} m. We arranged the molybdenum probe tips with a spacing of 1.7 mm to minimize the influence of the ion sheath. The oxide film of the molybdenum surface was removed with a wrapping sheet, because the oxide film was equivalent to a capacitor and a resistor, and the phase of the fluctuation changed. This advanced probe measurement system, which consisted of high speed Langmuir probes, was installed in TU-Heliac and its tips were laid on the same flux surface.

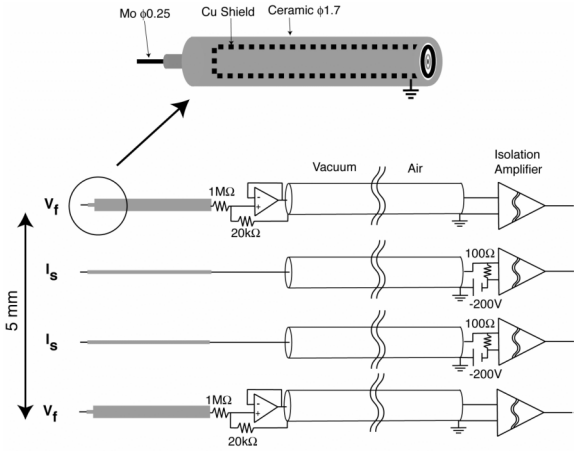

Fig. 1 Schematic diagram of floating potential V_f and ion saturation current I_s measurement system. Cutoff frequency of this system is 1 MHz.

3. Experimental Results

Biasing experiments were carried out and fluctuations were measured using the advanced probe measurement system at 3 radial positions, $\rho = 0.21$, 0.41, and 0.54, where $\rho = \langle r \rangle / a$, $\langle r \rangle$ was the average radius of the flux surface, and a was the minor radius of the last closed flux surface. The hot-cathode was positioned between $\rho = 0.18$ and 0.61. The hot-cathode bias voltage against the vacuum vessel was −230 V and the hot-cathode emission current was around −4 A. The power spectra of floating potential V_f fluctuation were calculated using the complex Fourier transform, as shown in Fig. 2. These spectra were normalized by the electron temperature measured with a triple probe. The unit of spectra was Hz^{-1}, and the relation between power spectra and root mean square (RMS) was:

$$\mathrm{RMS} = \sqrt{\int_0^\infty Power(f) df}. \quad (2)$$

From Fig. 2, we can divide the power spectra into 4 regions. The 1st region is the low frequency (LF) band ($f < 10$ kHz). The 2nd region is the medium frequency (MF) band ($10 < f < 50$ kHz). In this region, there are sharp spectra of fundamental and higher harmonics of ohmic heating (18 kHz). The 3rd region is the high frequency (HF) band ($70 < f < 200$ kHz). The 4th region is the band above 200 kHz. In this region, power decreases by a factor of $1/f^2$. The contribution of the 4th region to RMS

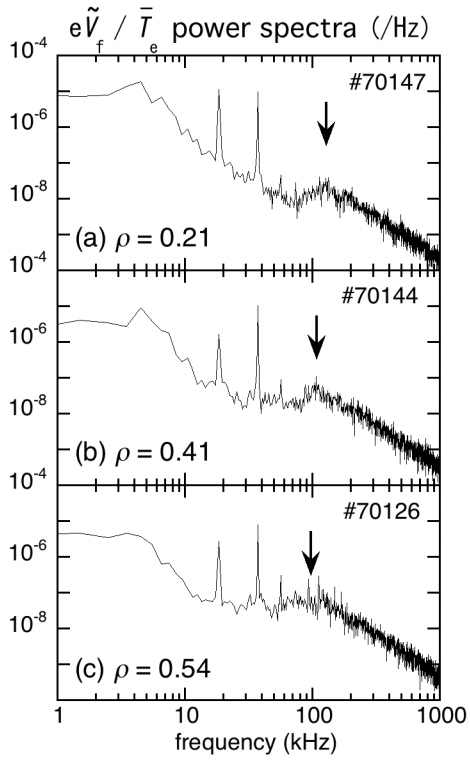

Fig. 2 Normalized power spectra of floating potential V_f at (a) $\rho = 0.21$, (b) $\rho = 0.41$ and (c) $\rho = 0.54$. Arrows indicate the peak position of the high frequency fluctuation.

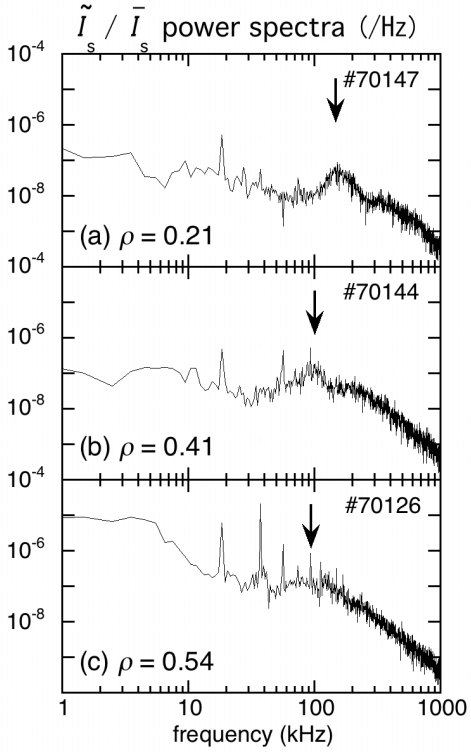

Fig. 3 Normalized power spectra of ion saturation current I_s at (a) $\rho = 0.21$, (b) $\rho = 0.41$ and (c) $\rho = 0.54$. Arrows indicate the peak position of the high frequency fluctuation.

can be neglected, and LF, MF, and HF power decide RMS. The frequency of the poloidal rotation estimated from the radial electric field was 50 ~ 100 kHz. In biased plasma, the phase velocity of the fluctuation was highly dependent on the poloidal flow velocity [13]. Then, poloidal mode of LF and MF fluctuations, the frequency of which was less than 50 kHz, should be 0. The arrows in Fig. 2 indicate the peak position of HF fluctuation. The peak position shifts to a higher frequency as the average radius ρ decreases. The cause of the shift may be the poloidal flow velocity difference inside and outside the plasma. The poloidal mode of HF fluctuation is expected to be 1, 2 or 3. From these results, the anomalous transport can be considered to be dominated by HF fluctuation, and not LF or MF fluctuations.

Power spectra of ion saturation current I_s fluctuation were also calculated, as shown in Fig. 3. The characteristics are the same as those of LF, MF, and HF fluctuations in V_f power spectra. However, there are small differences in the detailed characteristics between V_f and I_s power spectra. There are 2 peaks at $f = 150$ kHz and $f = 300$ kHz in the HF region in Fig. 3 (a). Power decreases by a factor of $1/f^{2\sim3}$ in the region above 200 kHz. The relations of V_f and I_s fluctuations in LF and HF are:

$$e\tilde{V}_f/T_e \geq \tilde{I}_s/I_s \ (LF), \tag{3}$$

$$e\tilde{V}_f/T_e \approx \tilde{I}_s/I_s \ (HF). \tag{4}$$

We can calculate the phase shift between 2 signals as follows. The time-dependent signal is transformed to a frequency-dependent signal using complex Fourier transform. The complex number contains its power and phase information. The difference in the argument of complex number between 2 signals is the phase shift. Figure 4 shows the phase shift between V_f and I_s fluctuations. At $\rho = 0.54$, the phase shift is almost 0 rad over all frequency ranges. On the other hand, at $\rho = 0.21$ the phase shift was detected, especially in the 100 ~ 200 kHz range.

Figure 5 shows time traces of V_f and I_s high frequency fluctuations. These were calculated with a digital high-pass filter using Fourier inverse transform for the region above 50 kHz. There are intermittent signals at $\rho = 0.21$. The order of the growth rate can be estimated as $10^5\ s^{-1}$ from the burst signal at time = 8.15 ms in Fig. 5 (a). The growth rate can be calculated from the dispersion relation. The growth rate of the drift wave was 10^3~$10^4\ s^{-1}$, and that of the flute mode, which was driven by the poloidal flow, was $10^5\ s^{-1}$ [11]. Hence, high frequency fluctuation at $\rho = 0.21$ may be the flute mode.

4. Summary

An advanced probe measurement system consisting of high speed Langmuir probes with a preamplifier and a Cu shield was designed and installed in TU-Heliac. Hot-

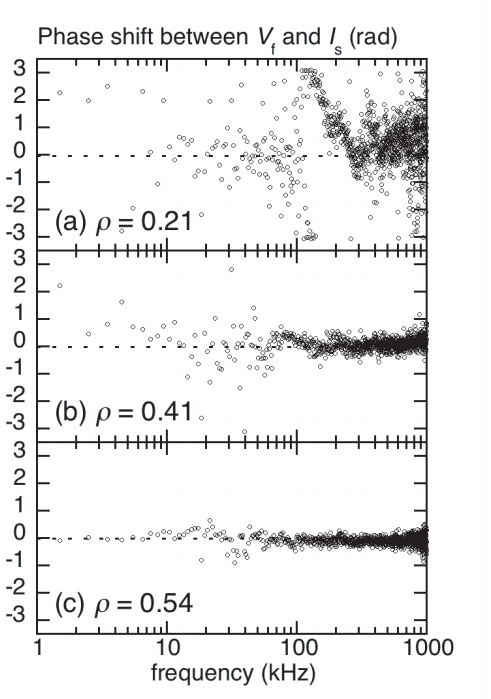

Fig. 4 Phase shift between V_f and I_s at (a) $\rho = 0.21$, (b) $\rho = 0.41$ and (c) $\rho = 0.54$.

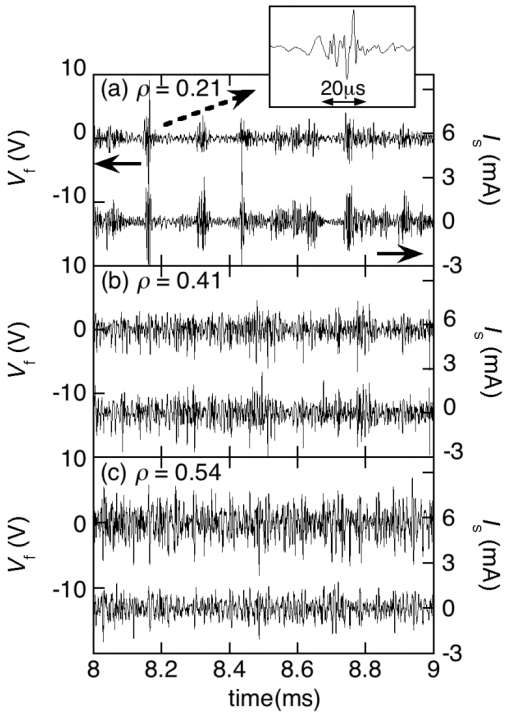

Fig. 5 Time traces of V_f and I_s high frequency fluctuations at (a) $\rho = 0.21$, (b) $\rho = 0.41$ and (c) $\rho = 0.54$. There are intermittent signals at $\rho = 0.21$. Growth rate can be estimated from the figure (a) as $10^5\,s^{-1}$.

cathode biasing experiments were carried out, and power spectra were calculated using complex Fourier transform. There were low frequency fluctuations ($f < 10$ kHz), high frequency fluctuations ($70 < f < 200$ kHz), and sharp spectra of ohmic heating ($10 < f < 50$ kHz). In the region above 200 kHz, the power of fluctuations decreased by a factor of $1/f^2$ for the potential fluctuation and $1/f^{2\sim3}$ for the density fluctuation. The phase shift between potential and density fluctuations was almost 0 rad at $\rho = 0.54$. On the other hand, the phase shift was detected at $\rho = 0.21$, especially in the $100 \sim 200$ kHz range. Time-dependent signals of high frequency fluctuation were obtained by Fourier inverse transform. The growth rate of high frequency fluctuation ($70 \sim 200$ kHz) at $\rho = 0.21$ was of the same order as flute mode. It was suggested that high frequency fluctuation was flute mode.

Acknowledgments

This work was supported by a Grant-in-Aid from the Ministry of Education, Science and Culture of Japan (No.17360439).

[1] F. Wagner *et al.*, Phys. Rev. Lett. **49**, 1408 (1982).
[2] F. Wagner *et al.*, Plasma Phys. Control. Fusion **36**, A61 (1994).
[3] S. Okamura *et al.*, Plasma Phys. Control. Fusion **46**, A113 (2004).
[4] R.J. Taylor *et al.*, Phys. Rev. Lett. **63**, 2365 (1989).
[5] E.Y. Wang *et al.*, Nucl. Fusion **35**, 467 (1995).
[6] C. Silva *et al.*, Nucl. Fusion **44**, 799 (2004).
[7] S. Kitajima *et al.*, J. Plasma Fusion Res. SERIES **4**, 391 (2001).
[8] Y. Tanaka *et al.*, J. Plasma Fusion Res. SERIES **6**, 371 (2004).
[9] H. Takahashi *et al.*, J. Plasma Fusion Res. SERIES **6**, 366 (2004).
[10] H. Takahashi *et al.*, Plasma Phys. Control. Fusion **48**, 39 (2006).
[11] Y. Tanaka *et al.*, Plasma Phys. Control. Fusion **48**, A285 (2006).
[12] S. Kitajima *et al.*, Plasma Phys. Control. Fusion **48**, A259 (2006).
[13] S. Kitajima *et al.*, Nucl. Fusion **46**, 200 (2006).